High-power terahertz radiation from surface-emitted THz-wave parametric oscillator*

Li Zhong-Yang(李忠洋)[a)b)†], Yao Jian-Quan(姚建铨)[a)b)], Xu De-Gang(徐德刚)[a)b)], Zhong Kai(钟 凯)[a)b)], Wang Jing-Li(汪静丽)[a)b)], and Bing Pi-Bin(邴丕彬)[a)b)]

[a)] College of Precision Instrument and Opto-electronics Engineering, Institute of Laser and Opto-electronics, Tianjin University, Tianjin 300072, China

[b)] Key Laboratory of Opto-electronics Information Science and Technology of Ministry of Education, Tianjin University, Tianjin 300072, China

(Received 18 November 2010; revised manuscript received 17 January 2011)

We report a pulsed surface-emitted THz-wave parametric oscillator based on two MgO:$LiNbO_3$ crystals pumped by a multi-longitudinal mode Q-switched Nd:YAG laser. Through varying the phase matching angle, the tunable THz-wave output from 0.79 THz to 2.84 THz is realized. The maximum THz-wave output was 193.2 nJ/pulse at 1.84 THz as the pump power density was 212.5 MW/cm^2, corresponding to the energy conversion efficiency of 2.42×10^{-6} and the photon conversion efficiency of about 0.037%. When the pump power density changed from 123 MW/cm^2 to 148 MW/cm^2 and 164 MW/cm^2, the maximum output of the THz-wave moved to the high frequency band. We give a reasonable explanation for this phenomenon.

Keywords: THz-wave parametric oscillator, noncollinear phase matching, THz-wave polarization, frequency tunable output

PACS: 42.65.Yj, 42.65.Dr, 42.65.Ky **DOI:** 10.1088/1674-1056/20/5/054207

1. Introduction

Recently the terahertz wave (THz-wave) generation technique has attracted much attention for its unique potential applications in material diagnostics, molecular analysis, remote atmospheric sensing and monitoring, real-time imaging and communication.[1−3] However, despite significant recent progress, the methods of generation of THz radiation are still less developed than that in the visible and the near-infrared regions, so the search for efficient, high-power, inexpensive, compact and room-temperature methods of generation of coherent THz radiation is one of the main topics in modern optoelectronics and photonics.[4,5] Among many electronic and optical methods for THz-wave generation, the THz-wave parametric oscillator (TPO) has many advantages, such as compactness, narrow linewidth, coherence, wide tunable range, high-power output and room temperature operation.[6,7] So far, distinctive TPO has been well developed in the past decade. On the phase matching side, the noncollinear phase matching and the quasi-phase-matched could satisfy the phase matching condition.[8,9] Considering the cavity design, the external cavity and the intracavity TPO could work well.[8,10] Regarding the THz-wave output, there are two methods. In the first method, in order to avoid the total reflection of THz-wave at the output side of MgO:$LiNbO_3$ crystal, the THz-wave is coupled out using a line of Si prisms.[9] It means that the THz-wave must undergo great loss and the beam quality is not good. The other method is to use the surface-emitted pattern to couple the THz-wave out.[11] In the surface-emitted TPO the THz-wave is coupled out perpendicularly to the exit surface of MgO:$LiNbO_3$ crystal without any output coupler, so the beam quality of THz-wave is good. Moreover, the generating area of THz-wave lies just under the exit surface of the MgO:$LiNbO_3$ crystal, the absorption loss of THz-wave to the crystal is low. For efficient generation of THz-wave based on the TPO, the MgO:$LiNbO_3$ crystal is one of the most suitable crystals due to its large nonlinear coefficient and high damage threshold.[12,13] Due to noncollinear phase matching in the TPO, the effective interaction volume of the three mixing waves (Pump, Stokes, THz-wave) is of vital importance for

*Project supported by the National Basic Research Program of China (Grant No. 2007CB310403), the National Natural Science Foundation of China (Grant No. 60801017), and the Research Fund for the Doctoral Program of Higher Education of China (Grant No. 20070420118).

†Corresponding author. E-mail: lzy8376@yahoo.com.cn

© 2011 Chinese Physical Society and IOP Publishing Ltd

the enhanced output of THz-wave. The pump wave with a larger beam radius can simultaneously generate the Stokes wave and the THz-wave with a larger beam radius, which results in a larger interaction volume of the three mixing waves.

In this work, the high-power THz-wave radiation was realized based on a surface-emitted TPO pumped by a multi-longitudinal mode Q-switched Nd:YAG laser. The frequency tuning characteristics of THz-wave agreed well with the theoretical curve calculated from the noncollinear phase matching condition. The maximum output of THz-wave moved to the high frequency band as the pump power density increased, which coincided with the theoretical analysis. As the pump power density was large enough, the third-order Stokes wave was observed.

2. Experimental setup

The schematic diagram of the TPO pumped by a multi-longitudinal mode Q-switched Nd:YAG laser is shown in Fig. 1. The nonlinear gain medium was composed of two 5 mol% MgO doped $LiNbO_3$ crystals. The dimensions of the rectangular crystal were $50(x)$ mm $\times$ $10(y)$ mm $\times$ $5(z)$ mm. The pentagonal crystal was cut from a rectangular crystal with dimensions of $65(x)$ mm $\times$ $17(y)$ mm $\times$ $5(z)$ mm and the cutting angles are shown in Fig. 1. The maximum length in the x-direction of the pentagonal crystal was 65 mm. All the end surfaces, which transmitted the pump wave, were polished and antireflection-coated for the pump wave and the Stokes wave. The pulse width, repetition rate and beam diameter of the pump wave were 15 ns, 10 Hz and 1.92 mm, respectively.

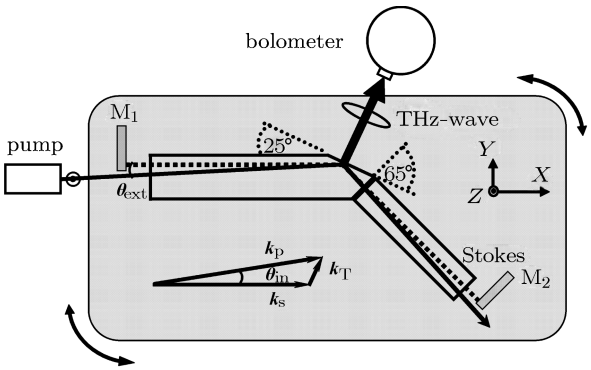


Fig. 1. Experimental setup of the MgO:$LiNbO_3$-TPO. The Fabry-perot cavity and the MgO:$LiNbO_3$ crystal were mounted onto a rotating stage.

The polarizations of the pump wave, the Stokes wave and the THz-wave were all along the z-axis of the MgO:$LiNbO_3$ crystal. The TPO cavity for the Stokes wave was formed by a pair of plane-parallel mirrors, M_1 and M_2. The M_1 was highly reflective in the infrared range, while the M_2 was coated to have a reflectivity of 95% in the infrared range. The cavity length was 215 mm. The pump wave passed through the cavity at the edges of M_1 and M_2. The cavity mirrors and the MgO:$LiNbO_3$ crystal were mounted on a rotating stage. The frequency tunable THz-wave radiation was obtained by rotating the stage continuously.

3. Results and discussion

During the polariton scattering process, the noncollinear phase matching condition $\boldsymbol{k}_\mathrm{p} = \boldsymbol{k}_\mathrm{s} + \boldsymbol{k}_\mathrm{T}$ and the conservation of energy $\omega_\mathrm{p} = \omega_\mathrm{s} + \omega_\mathrm{T}$ are satisfied, as can be seen in Fig. 1, where $\boldsymbol{k}_\mathrm{p}$, $\boldsymbol{k}_\mathrm{s}$ and $\boldsymbol{k}_\mathrm{T}$ are the wave vectors of the pump wave, the Stokes wave and the THz-wave, respectively. The incident angle of the Stokes wave to the exit facet of the THz-wave was 65°, which ensured the THz-wave was almost perpendicular to the exit from the $LiNbO_3$ crystal due to the noncollinear phase matching condition. The tunable THz-wave radiation can be obtained by continuously changing the angle θ_ext between the Stokes wave and the pump wave at the external side of the $LiNbO_3$ crystal. The tuning curve of the THz-wave radiation is shown in Fig. 2. The THz-wave frequency can be exactly figured out by using the energy conservation equation, since we have measured the wavelength of the Stokes wave. The THz-wave radiation from 0.8 THz to 2.8 THz was obtained. The experimental results agreed well with the values calculated from the noncollinear phase matching condition.

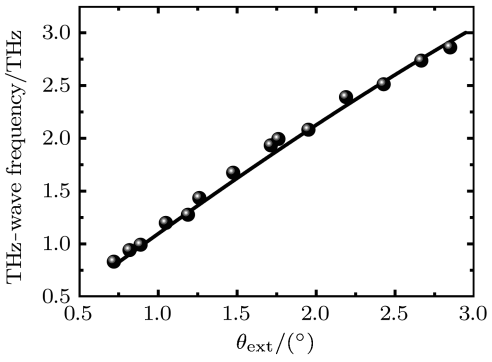


Fig. 2. Frequency tunable characteristics of the THz-wave. The θ_ext is the angle between the Stokes wave and the pump wave at the external side of crystal. The solid curve indicates the values calculated from the noncollinear phase matching condition and the dots indicate the experimental results.

The output characteristics of the THz-wave at the frequency of 1.84 THz as a function of the pump

power density is shown in Fig. 3. The THz-wave output was detected using silicon bolometer operating at temperature 4 K. We used transmittance-calibrated black polyethylene filters as the low-pass filters, which only allowed THz-wave to pass through. The threshold pump power density was about 54 MW/cm^2. The THz-wave power slowly increased at the threshold area and then quickly increased with the increase of the pump power density. When the pump power density was 212.5 MW/cm^2, the maximum output of the THz-wave was 193.2 nJ/pulse, corresponding to the energy conversion efficiency of 2.42×10^{-6} and the photon conversion efficiency of about 0.037%.

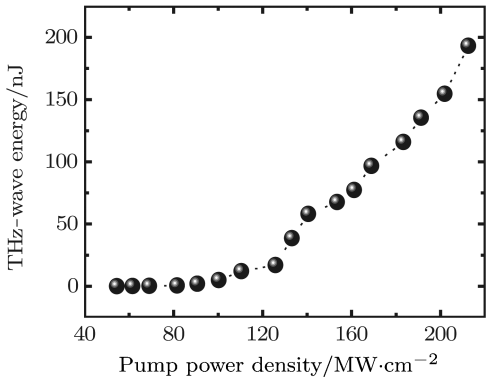


Fig. 3. THz-wave output as a function of the pump power density at 1.84 THz.

The tunable output of the THz-wave was obtained by rotating the stage on which the cavity and the MgO:LiNbO$_3$ crystals were fixed. Figure 4 shows the output characteristics of the THz-wave under pump power densities of 123 MW/cm^2, 148 MW/cm^2 and 164 MW/cm^2 respectively. We obtained a tunable THz-wave output from 0.79 THz to 2.84 THz when the pump power density was 164 MW/cm^2 and the maximum output of the THz-wave was 111 nJ. From the figure, we find that in the low frequency band the output of the THz-wave increases with the increase of frequency, while it drops drastically in the high frequency band. Two factors could account for this phenomenon. First, in the high frequency band, the increase of the phase matching angle will result in the decrease of the effective interaction volume of the three mixing waves. Second, the absorption coefficient of the MgO:LiNbO$_3$ crystal for the THz-wave is larger in the high frequency band. When the pump power density changed from 123 MW/cm^2 to 148 MW/cm^2 and 164 MW/cm^2, the frequencies corresponding to the maximum output of THz-wave were about 1.398 THz, 1.594 THz and 1.694 THz respectively.

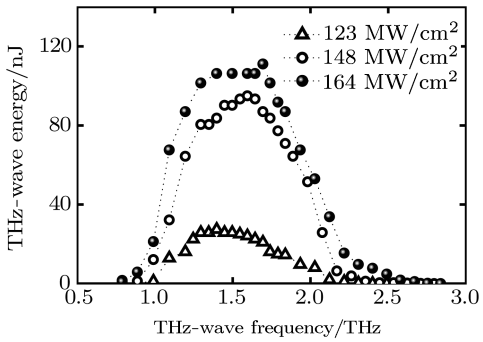


Fig. 4. THz-wave output characteristics at pump power densities of 123 MW/cm^2, 148 MW/cm^2 and 164 MW/cm^2 respectively.

The maximum value of THz-wave output moved to the high frequency band as the pump power density increased, which can be explained as follows. According to Ref. [14], the analytical expression of the exponential gain for the THz-wave is given by

$$\begin{aligned} g_{\mathrm{T}} &= g_{\mathrm{s}}\cos\varphi \\ &= \frac{\alpha_{\mathrm{T}}}{2}\left\{\left[1+16\cos\varphi\left(\frac{g_0}{\alpha_{\mathrm{T}}}\right)^2\right]^{1/2}-1\right\}, \end{aligned} \quad (1)$$

where α_{T} is the absorption coefficient in the THz range, φ is the phase-matching angle between the THz-wave and the pump wave and g_0 is the parametric gain in the low-loss limit. In the international system of units, they can be written as

$$g_0^2 = \frac{\omega_{\mathrm{s}}\omega_{\mathrm{T}}}{8\varepsilon_0 c n_{\mathrm{s}} n_{\mathrm{T}} n_{\mathrm{p}}} I_{\mathrm{p}}\left(d_{\mathrm{E}}+\sum_j \frac{S_j\omega_{0_j}^2 d'_{\mathrm{Q}_j}}{\omega_{0_j}^2-\omega_{\mathrm{T}}^2}\right)^2, \quad (2)$$

$$\begin{aligned} \alpha_{\mathrm{T}} &= 2\,|\mathrm{Im}\,k_{\mathrm{T}}| = 2\frac{\omega_{\mathrm{T}}}{c}\left|\mathrm{Im}\,\sqrt{\varepsilon(\omega_{\mathrm{T}})}\right| \\ &= 2\frac{\omega_{\mathrm{T}}}{c}\,\mathrm{Im}\left(\varepsilon_\infty+\sum_j \frac{S_j\omega_{0_j}^2}{\omega_{0_j}^2-\omega_{\mathrm{T}}^2-\mathrm{i}\,\omega_{\mathrm{T}}\Gamma_j}\right)^{1/2}, \end{aligned} \quad (3)$$

where ω_{0_j} and S_j are the eigenfrequency and the oscillator strength of the lowest A_1-symmetry phonon mode, respectively, coefficient $d_{\mathrm{E}} = 4d_{33}$ relates to the second-order nonlinear parametric processes, d'_{Q} relates to the third-order Raman scattering.

According to Eqs. (1)–(3), we calculated the absorption coefficient α_{T} and the THz-wave parametric gain coefficient g_{T} at 123 MW/cm^2, 148 MW/cm^2 and 164 MW/cm^2, which are shown in Fig. 5. The

gain coefficient g_T is about several cm^{-1} in the range from 0 to 3 THz and the absorption coefficient α_T increases monotonously to several tens of cm^{-1} with the increase of the frequency. The α_T is independent of the pump power density, so we just need to take into account the gain coefficient of the THz-wave when we qualitatively analyze the tunable output characteristics of the THz-wave for different pump power densities. From the figure, we find that when the pump power density changes from 123 MW/cm^2 to 148 MW/cm^2 and 164 MW/cm^2, the maximum gain of the THz-wave moves to the high frequency band. Because the absorption coefficients α_T are equal at the same frequency for the three curves, the maximum value of the THz-wave output moves to the high frequency band when the other conditions are identical, which is what we find in Fig. 4.

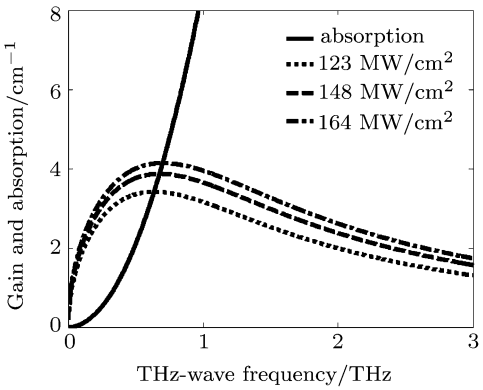


Fig. 5. THz-wave absorption and parametric gain coefficient at 123 MW/cm^2, 148 MW/cm^2 and 164 MW/cm^2.

When the phase matching angle θ_{in} was 0.79° and the pump power density was 150 MW/cm^2, we observed the radiations of the first-order, the second-order and the third-order Stokes waves, as shown in Fig. 6. From the figure, we find that the frequency shift between neighbour order Raman scatterings is approximately the same, which corresponds to the frequency of the generated THz-wave. When the pump power density was large enough, the first-order Stokes wave interacted with the stimulated polariton to generate the second-order Stokes wave and the THz-wave with frequency corresponding to the difference between the first-order and the second-order Stokes waves.

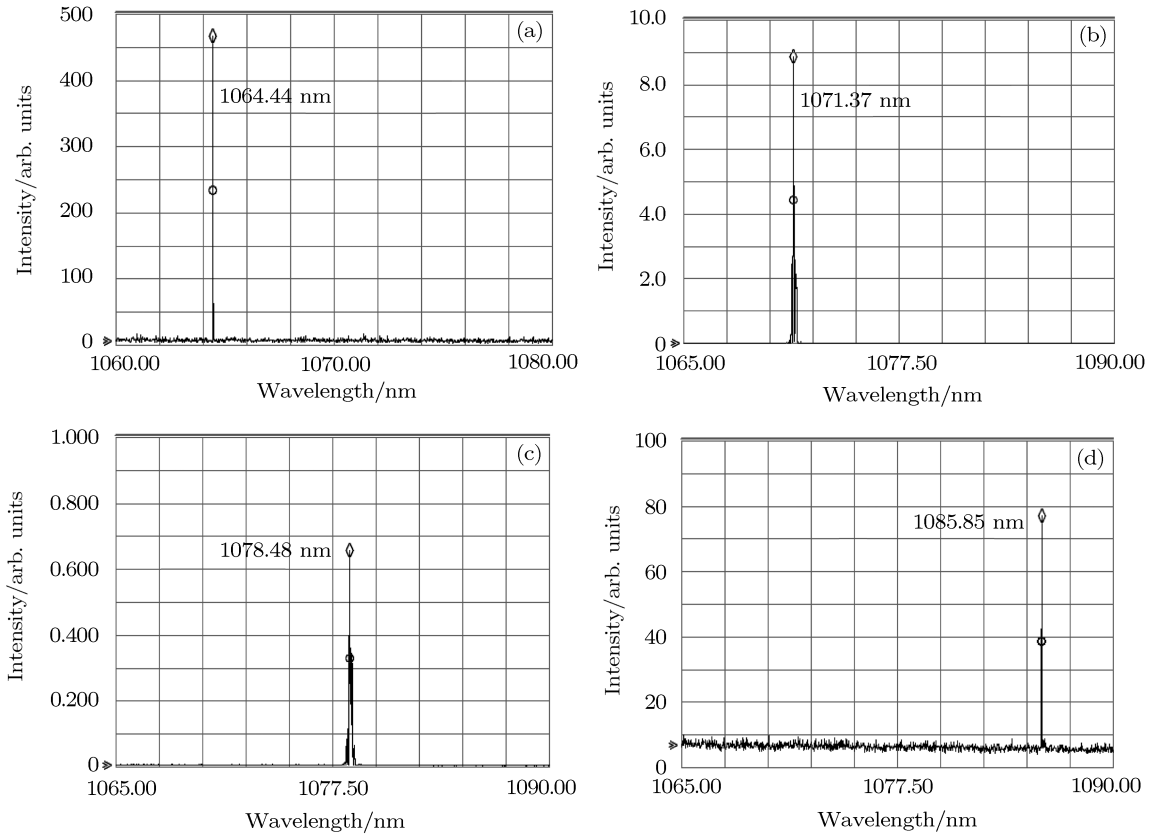


Fig. 6. The spectra of the pump and the Stokes waves. (a) The pump wave, (b) the first-order Stokes wave, (c) the second-order Stokes wave, (d) the third-order Stokes wave.

4. Conclusion

The high-power THz-wave radiation from the surface-emitted TPO based on MgO:$LiNbO_3$ crystals was obtained. We analyzed the tunable characteristics of the surface-emitted TPO. By varying the phase matching angle, a tunable THz-wave from 0.79 THz to 2.84 THz was obtained. When the pump power density was 212.5 MW/cm^2, the maximum THz-wave output was 193.2 nJ/pulse at 1.84 THz, corresponding to the energy conversion efficiency of 2.42×10^{-6} and the photon conversion efficiency of about 0.037%. When the pump power density changed from 123 MW/cm^2 to 148 MW/cm^2 and 164 MW/cm^2, the frequencies corresponding to maximum output of the THz-wave were about 1.398 THz, 1.594 THz and 1.694 THz, respectively. When $\theta_{\rm in}$ was 0.79° and the pump power density was 150 MW/cm^2, we observed the first-order, the second-order and the third-order Stokes waves.

Acknowledgements

The authors thank the Hiromasa Ito team of PDC RIKEN for their guidance on this work.

References

[1] Siegel P 2002 *IEEE Trans. Microwave Theory Tech.* **50** 910
[2] Kawase K, Ogawa Y, Watanabe Y and Inoue H 2003 *Opt. Express* **11** 2549
[3] Hu M, Zhang Y X, Yan Y, Zhong R B and Liu S G 2009 *Chin. Phys.* B **18** 3877
[4] Kuznetsova E, Rostovtsev Y, Kalugin N G, Kolesov R, Kocharovskaya O and Scully M O 2006 *Phys. Rev.* A **74** 023819
[5] Suizu K and Kawase K 2007 *Opt. Lett.* **32** 2990
[6] Sun B, Liu J S, Li E B and Yao J Q 2009 *Chin. Phys.* B **18** 2846
[7] Guo R X, Akiyama K and Minamide H 2007 *Appl. Phys. Lett.* **90** 121127
[8] Kawase K, Shikata J, Imai K and Ito H 2001 *Appl. Phys. Lett.* **78** 2819
[9] Molter D, Theuer M and Beigang R 2009 *Opt. Express* **17** 6623
[10] Edwards T, Walsh D, Spurr M, Rae C and Dunn M 2006 *Opt. Express* **14** 1582
[11] Ikari T, Zhang X B, Minamide H and Ito H 2006 *Opt. Express* **14** 1604
[12] Xu G, Mu X, Ding Y J and Zotova I B 2009 *Opt. Lett.* **34** 995
[13] Yeh K L, Hoffmann M C, Hebling J and Nelson K A 2007 *Appl. Phys. Lett.* **90** 171121
[14] Sussman S S 1970 *Report of Microwave Lab, Stanford University* No. 1851